arXiv:1411.7020v1 [math-ph] 25 Nov 2014

The dilute Temperley-Lieb O($n = 1$) loop model on a semi infinite strip: the ground state

A. Garbali[1] and B. Nienhuis[2]

[1]LPTHE, CNRS UMR 7589,
Université Pierre et Marie Curie (Paris 6),
4 place Jussieu, 75252 Paris cedex 05, France.

[2]Instituut voor Theoretische Fysica,
Universiteit van Amsterdam, Science Park 904,
1098 XH Amsterdam, The Netherlands.

Abstract

We consider the integrable dilute Temperley-Lieb (dTL) O($n = 1$) loop model on a semi-infinite strip of finite width L. In the analogy with the Temperley-Lieb (TL) O($n = 1$) loop model the ground state eigenvector of the transfer matrix is studied by means of a set of q-difference equations, sometimes called the qKZ equations. We compute some ground state components of the transfer matrix of the dTL model, and show that all ground state components can be recovered for arbitrary L using the qKZ equation and certain recurrence relation. The computations are done for generic open boundary conditions.

1 Introduction

In the last decade the integrable loop models with the loop weight $n = 1$ became a subject of great interest due to their relation to combinatorics, algebraic geometry, percolation, etc. Probably, the most striking result is the Razumov-Stroganov (RS) conjecture, relating the components of the ground state of the TL loop model to alternating sign matrices [1, 22]. The weaker version of this conjecture [1] was proved in [12], while the stronger RS conjecture [22] in [4]. The ground state of the TL loop model is known to be related to certain orbital varieties. Namely, the entries of the ground state of the TL loop model coincide with the multidegrees of certain matrix varieties [12, 17]. The TL loop model at $n = 1$ is equivalent to critical bond percolation. Studying the ground state of the TL model with different boundary conditions allows to compute some correlation functions for critical bond percolation [19, 18]. Since the O(1) TL loop model appears to be very fruitful it motivates us to study also the dilute TL loop model.

When the loop weight $n = 1$, the dTL loop model is related to critical site percolation. Hence, the knowledge of its ground state can be helpful for the computation of correlation

functions for critical site percolation. At $n = 0$ the ground state of the dTL model may provide a method to approach the closed self avoiding walk in 2D. In both cases ($n = 1$ and $n = 0$) the scaling limits are described by a Schramm-Loewner evolution (SLE). It is, however, a conjecture for the self avoiding walk. The dTL loop model at finite size may provide insights to the relations to SLE.

The loop model we discuss here is defined on the square lattice which is finite in width and infinite in length. This domain can be seen as a half infinite strip that has two vertical half infinite boundaries and one finite horizontal boundary of length L. We may identify the vertical boundaries, this will lead to periodic boundary conditions. We can also allow any configuration at the vertical boundaries which will lead to open boundary conditions. The configurations of the dTL model can be labeled by the connectivities of the links on the horizontal boundary. Each edge of the horizontal boundary can be in two states: occupied or unoccupied. An occupied edge is connected to another edge on the horizontal boundary. This way each configuration of the model corresponds to a link pattern on the horizontal boundary. All link patterns form a vector space lp_L, thus the states of the model can be expressed in this vector space. An important idea that lead to many advances for the TL model is to consider more general lattices, i.e. lattices with distortions or inhomogeneities $z_1, .., z_L$. When the loop weight is equal to 1, the ground state configuration Ψ_L becomes a vector with polynomial in z_i entries which satisfy certain q-difference equations sometimes referred to as the quantum Knizhnik-Zamolodchikov equations (qKZ). A crucial ingredient for the computations is the conjectural expression for a certain entry of the ground state. Using this conjecture all other elements follow from the qKZ equations. This was the basis of the algorithm for the computation of the ground state components and the sum rules for the TL O(1) loop models with various boundary conditions [12, 11, 26, 7, 3] and for the dTL O(1) model with periodic boundary conditions [10]. We extend these results to the dTL O(1) model with open boundary conditions.

We organize the paper as follows. In the second section we present the definitions and the basic ingredients. In the section 3 we set the loop weight to 1 and study the qKZ equations, after we discuss the recurrence in size and finally compute the ground state. Discussions follow in the section 4. The explicit results for Ψ_L for $L = 1$ and 2 are given in the appendix A. Appendix B contains the discussion of the recurrence relation.

2 The dilute O(n) loop model

2.1 Link pattern basis and the R-matrix

The dilute O(n) loop model is defined on the square lattice on a semi-infinite strip. An example of a configuration of the model is given on the fig.(1). The loops may end at the horizontal boundary and two vertical boundaries. We are going to classify all configurations according to their connectivity on the horizontal boundary, such a connectivity is called a link pattern. More precisely, let us label the edges of the lower boundary with numbers $1, 2, .., L$ from left to right. If a loop ends at an edge i, then this edge is said to be occupied, if there are no loops ending at this edge, then this edge is unoccupied. Moreover, we will distinguish the occupied edges according to their connectivity with the edges (or the vertical boundaries) on its left and on its right. It is convenient to label the connectivity n_i of an edge

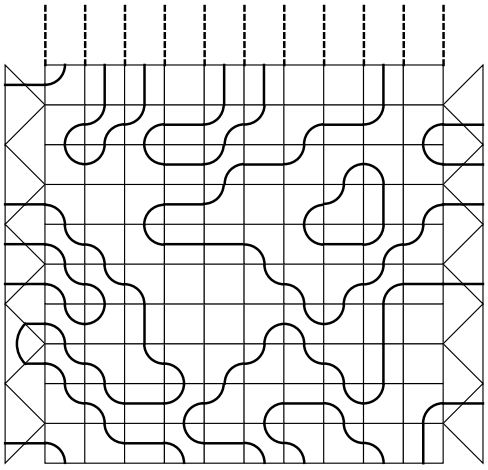

Figure 1: A typical configuration of the dilute O(n) loop model on a fragment of a semi-infinite strip.

i by -1, 0 or 1. In a given configuration to an unoccupied edge i we assign $n_i = 0$, an edge i occupied and connected to an edge or a boundary on its right will get $n_i = 1$, finally to an edge i that is occupied by a line that ends on its left we assign $n_i = -1$. With this notation the connectivity of a configuration is the set $\{n_1, n_2, .., n_L\}$. For example, the configuration depicted on fig.(1) has the connectivity $\{-1, 0, 0, -1, 0, 1, 1, 0, -1, 1\}$. We can represent this pictorially as on fig.(2), where the vertical boundaries are represented by the leftmost and the rightmost points separated by a dashed line from the actual horizontal boundary. The set of all link patterns, denoted by lp_L, is the basis in which we express the eigenvectors of the transfer matrix of the model.

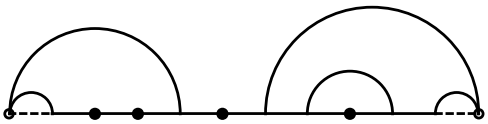

Figure 2: The link pattern that corresponds to the configuration from the fig.(1).

Now we define the set of operators which act in the space lp_L of the link patterns of length L. Graphically these operators are defined by the plaquettes of the fig.(3).

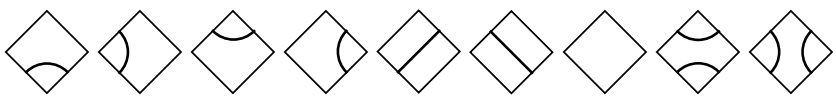

Figure 3: The operators acting on the link patterns.

We will label these operators by $\rho^{(1)}, \rho^{(2)}, .., \rho^{(9)}$ in the order given in fig.(3). By $\rho_j^{(i)}$ we will denote the action of the operator $\rho^{(i)}$ on two adjacent sites j and $j+1$ of a link pattern. It is better to describe graphically the action of these operators as on fig.(4).

The action of $\rho^{(i)}$ on the link patterns should respect the occupation, i.e., the top left and top right occupations of a $\rho_j^{(i)}$ should coincide with the occupations of the edges j and

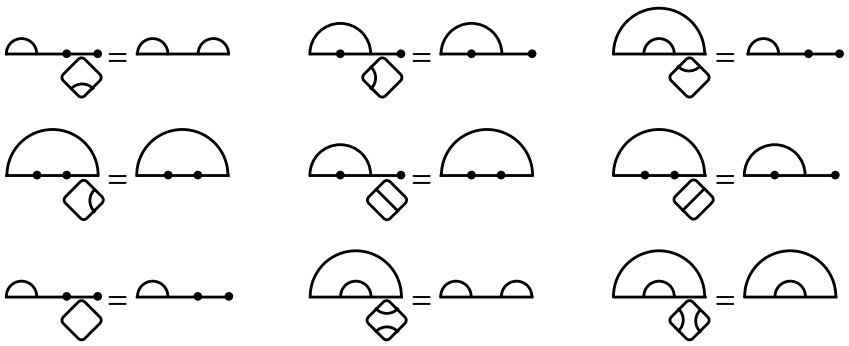

Figure 4: Here we present few link patterns on which $\rho^{(i)}$ operators act.

$j+1$ (respectively) in the link pattern, otherwise the action gives zero. We notice that $\rho^{(2)}, \rho^{(4)}, \rho^{(7)}$ and $\rho^{(9)}$ act as identity operators, $\rho^{(5)}$ and $\rho^{(6)}$ act locally interchanging an occupied edge with an unoccupied edge, the operator $\rho^{(1)}$ also acts locally by inserting a little arch at the position $j,\ j+1$ of a link pattern. The two remaining operators $\rho^{(3)}$ and $\rho^{(8)}$, as we can see, change the global picture. Moreover, $\rho^{(3)}$ and $\rho^{(8)}$ may produce a loop or a boundary to boundary link as on the fig(5). We can erase the closed loops by the cost of its weight n and the boundary to boundary link by the cost of its weight n_0.

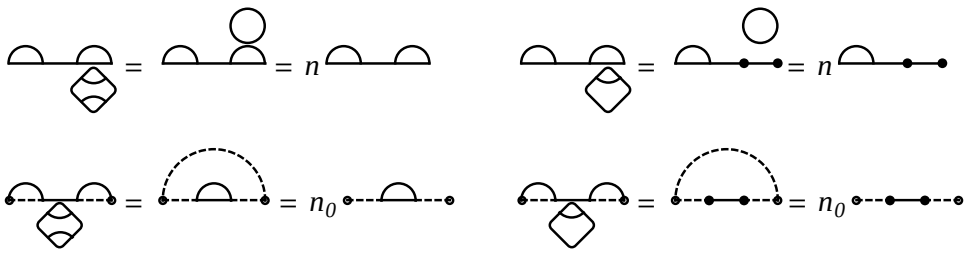

Figure 5: The operators $\rho^{(3)}$ and $\rho^{(8)}$ produce a closed loop or a line connecting two vertical boundaries, the line is represented by a dashed semi-circle.

At this point we can turn to the integrability. In order to do this we introduce the $\check{R}$-matrix (operator) which is a weighted sum of all nine operators $\rho_j^{(i)}$ (see fig.(6))

$$\check{R}_j(z_j, z_{j+1}) = \sum_{i=1}^{9} \rho_j^{(i)} r_i(z_j, z_{j+1}). \tag{1}$$

The operator $\check{R}_j(z_j, z_{j+1})$ acts non trivially on the j-th and $j+1$-st space which carry the

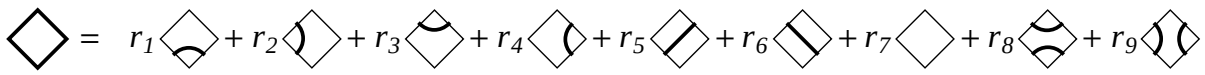

Figure 6: $\check{R}$-operator.

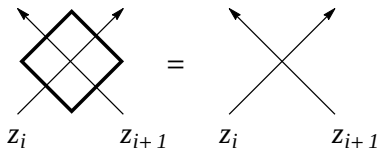

Figure 7: The $\check{R}_i(z_i, z_{i+1})$-operator.

rapidities z_j and z_{j+1} respectively, on the rest of the lattice spaces it acts as identity. In the graphical notation the rapidities are carried by the oriented straight lines as on fig.(7).

The integrable dilute O(n) loop model is defined by the $\check{R}$-operator that satisfies the Yang-Baxter (YB) equation [2]. The $\check{R}$-matrix, in fact, depends only on the ratio of the two spectral parameters so we may write $\check{R}_j(z_{j+1}/z_j) \propto \check{R}_j(z_j, z_{j+1})$, then the YB equation reads:

$$\check{R}_{i+1}(z/y)\check{R}_i(z/x)\check{R}_{i+1}(y/x) = \check{R}_i(y/x)\check{R}_{i+1}(z/x)\check{R}_i(z/y). \tag{2}$$

Graphically it is shown on the fig.(8). This equation gives the constraints on the weights

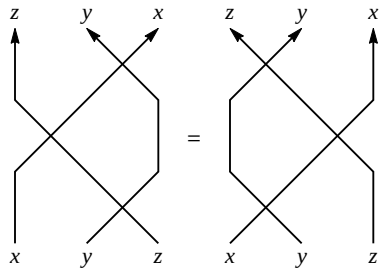

Figure 8: The Yang-Baxter equation.

$r_i(z)$. The integrable R-operator was obtained in [21, 20]. In the, so called, additive notation the weights are:

$$\begin{aligned}
&r_1(x) = r_3(x) = \sin 2\lambda \sin(3\lambda - x), \quad r_2(x) = r_4(x) = \sin 2\lambda \sin x, \\
&r_5(x) = r_6(x) = \sin x \sin(3\lambda - x), \quad r_7(x) = \sin x \sin(3\lambda - x) + \sin 2\lambda \sin 3\lambda \\
&r_8(x) = \sin(2\lambda - x) \sin(3\lambda - x), \quad r_9(x) = -\sin x \sin(\lambda - x),
\end{aligned} \tag{3}$$

and the loop weight is expressed through the loop fugacity λ:

$$n = -2\cos 4\lambda. \tag{4}$$

For our purposes the multiplicative notation is more appropriate (which we already implied above). In this case we set: $z = e^{ix}$ and $q = e^{i\lambda}$ in (3), so (up to a common factor) we have:

$$\begin{aligned}
&r_1(z) = r_3(z) = -\left(q^4 - 1\right) z \left(q^6 - z^2\right), \quad r_2(z) = r_4(z) = -q^3 \left(q^4 - 1\right) z \left(z^2 - 1\right), \\
&r_5(z) = r_6(z) = -q^2 (z^2 - 1) \left(q^6 - z^2\right), \quad r_7(z) = q^8 + q^2 z^4 - \left(q^2 + 1\right) \left(q^8 - q^4 + 1\right) z^2, \\
&r_8(z) = q^4 \left(z^2 - 1\right) \left(q^2 - z^2\right), \quad r_9(z) = -\left(q^4 - z^2\right) \left(q^6 - z^2\right).
\end{aligned} \tag{5}$$

Another operator that we will use is the $R_i(z)$ matrix. It is simply the $\check{R}$ tilted by 45 degrees.

2.2 Open boundary conditions

By the boundary of the half infinite strip we understand the two half infinite vertical lines. One may consider then the periodic boundary conditions, i.e. when the two vertical boundaries are identified, closed boundary conditions, i.e. when the loops are reflected from the vertical boundaries. For general non periodic boundary conditions the loops may end at both vertical boundaries. One can also consider open boundary conditions with certain restrictions and various mixed boundary conditions. This is better discussed in [13]. In the case of general open boundary conditions the left and the right boundaries carry the boundary spectral parameters. In the conclusion we will mention how to recover the ground states corresponding to the other non periodic boundary conditions from the ground state corresponding to the general open boundary conditions considered here.

Now we introduce the boundary operators. These operators act on the leftmost and the rightmost points of the link patterns. Graphically they are defined by the plaquettes on fig.(9). We denote the left boundary operators by $\kappa_l^{(1)}, ..\kappa_l^{(5)}$ and the right boundary

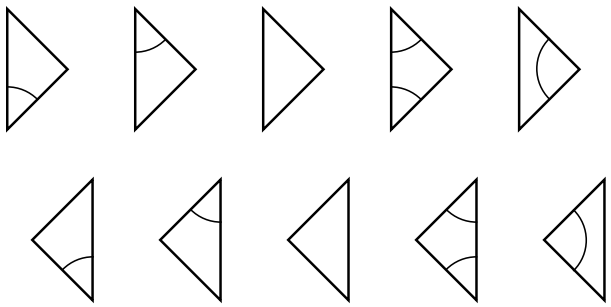

Figure 9: The left and the right boundary operators.

operators by $\kappa_r^{(1)}, .., \kappa_r^{(5)}$, ordered as on the picture (9). Few examples of their action on link patterns are presented on fig.(10).

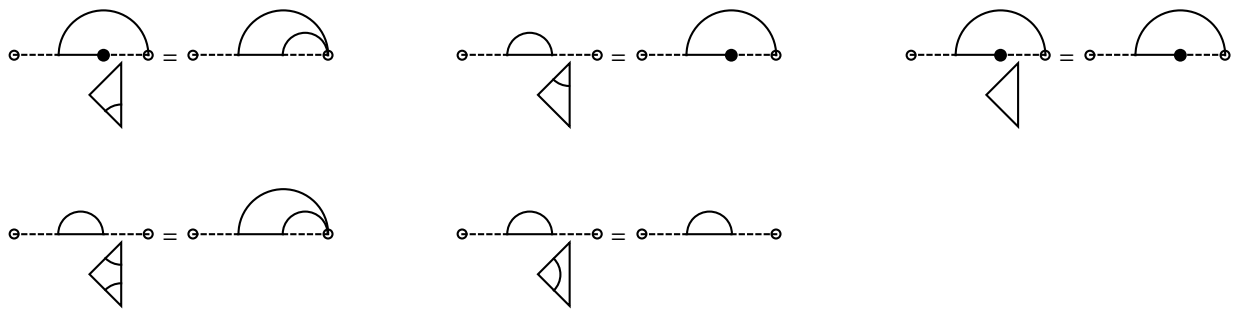

Figure 10: The action of the κ_r-operators.

We introduce the K_l-matrix for the left boundary and the K_r-matrix for the right boundary. The K-matrices represent the weighted action of the κ operators with the weights: $k_i(z_1, \zeta_l)$ for the left K-matrix and $k_i(z_L, \zeta_r)$ for the right K-matrix. Here, ζ_l and ζ_r are the

left and the right boundary rapidities, hence the left and right (fig.(11)) K-operators are:

$$K_l(z_1,\zeta_l)=\sum_{i=1}^{5}\kappa_l^{(i)}k_i(z_1,\zeta_l),\quad K_r(z_L,\zeta_r)=\sum_{i=1}^{5}\kappa_r^{(i)}k_i(z_L,\zeta_r). \tag{6}$$

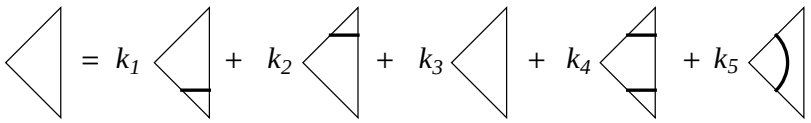

Figure 11: The right K-operator.

The action of $K_i(z,\zeta)$ switches the rapidity from z to $1/z$. The corresponding graphical notation for $K_r(z_L,\zeta_r)$ is shown on fig.(12). In order to preserve the integrability we need to

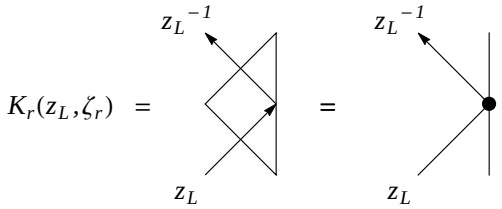

Figure 12: The operator $K_r(z_L,\zeta_r)$.

impose certain conditions on the k's, namely the boundary Yang-Baxter (BYB) equation [24]. For the right boundary it is shown graphically on the fig.(13) and reads:

$$\check{R}_{L-1}(w/z)K_r(z,\zeta_r)\check{R}_{L-1}(1/(wz))K_r(w,\zeta_r)=K_r(w,\zeta_r)\check{R}_{L-1}(1/(wz))K_r(z,\zeta_r)\check{R}_{L-1}(w/z). \tag{7}$$

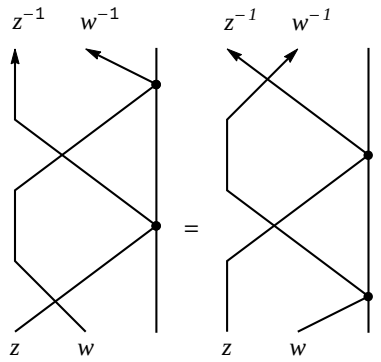

Figure 13: The boundary Yang-Baxter equation.

The integrable boundary weights for the right boundary K-matrix in the additive con-

vention are the following [8, 5]:

$$
\begin{aligned}
&k_1(x,\zeta) = k_2(x,\zeta) = \zeta \sin 2\lambda \sin 2x,\\
&k_3(x,\zeta) = 2\cos\lambda \sin(\frac{3}{2}\lambda + x) - \zeta^2 n_0 \sin(\frac{1}{2}\lambda + x)\sin(\frac{1}{2}\lambda - x)\sin(\frac{3}{2}\lambda - x),\\
&k_4(x,\zeta) = -\zeta^2 \sin 2\lambda \sin 3x \sin(\frac{1}{2}\lambda - x),\\
&k_5(x,\zeta) = \sin(\frac{3}{2}\lambda - x)(2\cos\lambda - \zeta^2 n_0 \sin^2(\frac{1}{2}\lambda - x)),
\end{aligned}
\tag{8}
$$

here n_1 is the weight of a loop ending on two boundary points. There is a different solution to the reflection equation, for more details see [5].

In the multiplicative convention: $z = e^{ix}$ and $q = e^{i\lambda}$ in (8), the weights read:

$$
\begin{aligned}
&k_1(z,\zeta) = k_2(z,\zeta) = -\frac{\zeta\,(q^4-1)\,(z^4-1)}{4q^2z^2},\\
&k_3(z,\zeta) = \frac{i\,(\zeta^2 n_0\,(q-z^2)\,(q^3-z^2)\,(qz^2-1) + 4\,(q^2+1)\,z^2\,(q^3z^2-1))}{8q^{5/2}z^3},\\
&k_4(z,\zeta) = \frac{i\zeta^2\,(q^4-1)\,(z^4-1)\,(q-z^2)}{8q^{5/2}z^3},\\
&k_5(z,\zeta) = \frac{i\,(q^3-z^2)\left(\zeta^2 n_0\,(q-z^2)^2 + 4\,(q^2+1)\,z^2\right)}{8q^{5/2}z^3}.
\end{aligned}
\tag{9}
$$

The transfer operator $T(t|z_1,..,z_L;\zeta_l,\zeta_r)$, depicted on the fig.(14), is an operator acting in the space of link patterns. It is constructed from the R and K matrices:

$$
T(t|z_1,..,z_L;\zeta_l,\zeta_r) = Tr\big(R_1(t,z_1)..R_L(t,z_L)K_r(t,\zeta_r)R_L(z_L,t^{-1})..R_L(z_1,t^{-}1)K_l(t^{-1},\zeta_l)\big),
\tag{10}
$$

where the trace means that the lower edge of the $K_l(t^{-1},\zeta_l)$ needs to be identified with the left edge of $R_1(t,z_1)$. Due to the YB and the BYB two transfer matrices with different values of t commute:

$$
[T(t_1), T(t_2)] = 0.
\tag{11}
$$

Other important properties of the transfer matrix coming from the YB and BYB are the commutations with the $\check{R}$:

$$
T(t|z_1,..,z_i,z_{i+1},..,z_L;\zeta_l,\zeta_r)\check{R}_i(z_i,z_{i+1}) = \check{R}_i(z_i,z_{i+1})T(t|z_1,..,z_{i+1},z_i,..,z_L;\zeta_l,\zeta_r),
\tag{12}
$$

and with the K-matrix:

$$
K_l(1/z_1,\zeta_l)T(t|1/z_1,z_2,..,z_L;\zeta_l,\zeta_r) = T(t|z_1,z_2,..,z_L;\zeta_l,\zeta_r)K_l(1/z_1,\zeta_l),
\tag{13}
$$

$$
K_r(1/z_L,\zeta_r)T(t|z_1,..,z_{L-1},1/z_L;\zeta_l,\zeta_r) = T(t|z_1,...z_{L-1},z_L;\zeta_l,\zeta_r)K_r(1/z_L,\zeta_r)
\tag{14}
$$

The common ground-state vector of the family of transfer matrices $T(t|z_1,..,z_L;\zeta_l,\zeta_r)$ parametrized by t we denote by Ψ_L:

$$
T(t|z_1,..,z_L;\zeta_l,\zeta_r)\Psi_L(z_1,..,z_L;\zeta_l,\zeta_r) \propto \Psi_L(z_1,..,z_L;\zeta_l,\zeta_r).
\tag{15}
$$

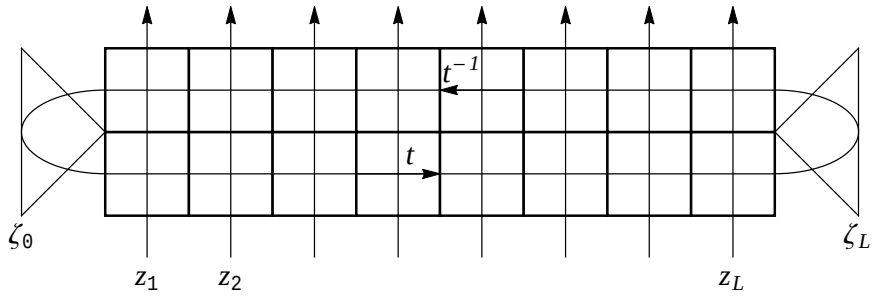

Figure 14: The graphical representation of the transfer operator.

The eigenvectors of T can be written in the link pattern basis, in particular:

$$\Psi_L(z_1,..,z_L;\zeta_l,\zeta_r) = \sum_{\pi\in \mathrm{LP}_L} \psi_\pi(z_1,..,z_L;\zeta_l,\zeta_r)|\pi\rangle. \tag{16}$$

Our aim is to understand how to compute the components ψ_π when the loop weight n (and also n_0) is equal to 1.

3 Loop weight $n = 1$

In this section we specify our model to the case when $q^3 = -1$, then the loop weight n (and we assume also $n_0 = n$) have the weight equal to 1. This means that the presence of the closed loops in a configuration does not affect the weight of this configuration. At this point the ground state is a steady state of the stochastic process defined by the Hamiltonian (or transfer matrix) of the system. The ground state entries become the relative probabilities of the occurrence of the corresponding link patterns. Assuming that the transfer matrix is normalized, the ground state eigenvector equation becomes:

$$T(t|z_1,..,z_L;\zeta_l,\zeta_r)\Psi_L(z_1,..,z_L;\zeta_l,\zeta_r) = \Psi_L(z_1,..,z_L;\zeta_l,\zeta_r). \tag{17}$$

Which means the invariance of the probabilities under the addition of two rows of the transfer matrix. Since the transfer matrix is a rational function of the rapidities, we can normalize Ψ_L such that its all components are coprime polynomials.

We will replace everywhere q by ω and assume $\omega^3 = -1$. The R and K-matrices simplify:

$$\begin{aligned} &r_1(z) = r_2(z) = r_3(z) = r_4(z) = \omega(\omega+1)z, \quad r_5(z) = r_6(z) = r_7(z) = z^2-1, \\ &r_8(z) = -(\omega+z)\left(\omega^2 z+1\right), \quad r_9(z) = \left(\omega^2+z\right)(\omega z+1). \end{aligned} \tag{18}$$

$$\begin{aligned} &k_{1,l}(z,\zeta_l) = k_{2,l}(z,\zeta_l) = -\frac{(\omega+1)(z^2-1)}{z}, \quad k_{3,l}(z,\zeta_l) = \frac{\zeta^2\omega+\zeta^2\omega z^4-\zeta^2\omega z^2+z^2}{\zeta z^2}, \\ &k_{4,l}(z,\zeta_l) = -\frac{\zeta(\omega+1)(z^2-1)(\omega-z^2)}{z^2}, \quad k_{5,l}(z,\zeta_l) = -\frac{(-\zeta\omega+\zeta z^2-z)(-\zeta\omega+\zeta z^2+z)}{\zeta z^2}. \end{aligned} \tag{19}$$

The weights of the right boundary K-matrix are given by $k_{i,r}(z,\zeta) = k_{i,l}(1/z,\zeta)$.

The result of the action of the $\check{R}$ matrix on a link pattern is the sum of the link patterns obtained from the action of the $\rho^{(j)}$ operators, weighted by the r_j's respectively. For example, on a link pattern with two empty sites $n_i = 0,\ n_{i+1} = 0$, $\check{R}_i$ acts by $\rho^{(1)}$ with the probability r_1 and by $\rho^{(7)}$ with the probability r_7. Hence, we need to normalize this action with $W = r_1 + r_7$. In fact, the weights (18) are such that for any occupation n_i and n_{i+1} the normalization is the same.

$$W(z_i, z_{i+1}) = (\omega z_i + z_{i+1}) \left(\omega^2 z_i + z_{i+1}\right). \tag{20}$$

Similar arguments apply to the K-matrices. The normalizations of K_l and K_r are:

$$U_l(z, \zeta_l) = -\frac{(\omega\zeta_l - z^2\zeta_l + z)\,(-\zeta_l + \omega z^2\zeta_l - z)}{z^2\zeta_l}, \tag{21}$$

$$U_r(z, \zeta_r) = \frac{(-\omega\zeta_r + z^2\zeta_r + z)\,(-\zeta_r + \omega z^2\zeta_r + z)}{z^2\zeta_r}. \tag{22}$$

Now, using the eq.(12) we find: 0

$$\check{R}(z_i, z_{i+1})\Psi_L(z_1, .., z_i, z_{i+1}, .., z_L; \zeta_l, \zeta_r) = W(z_i, z_{i+1})\Psi_L(z_1, .., z_{i+1}, z_i, .., z_L; \zeta_l, \zeta_r), \tag{23}$$

and also, using the eq.(13) and eq.(14):

$$K_l(z_1, \zeta_l)\Psi_L(z_1, .., z_L; \zeta_l, \zeta_r) = U_l(z_1, \zeta_l)\Psi_L(1/z_1, .., z_L; \zeta_l, \zeta_r), \tag{24}$$

$$K_r(z_L, \zeta_r)\Psi_L(z_1, .., z_L; \zeta_l, \zeta_r) = U_r(z_L, \zeta_r)\Psi_L(z_1, .., 1/z_L; \zeta_l, \zeta_r). \tag{25}$$

Equations (23)-(25) together will be called the qKZ equations. This set of equations is a system of functional equations with polynomial solutions. It allows to find all components of the ground state only if a certain set of the components is already known. These components ψ_π are those which correspond to the link patterns $\pi_i = \{0_1, .., 0_i, -1_{i+1}, .., -1_L\}$ or $\tilde{\pi}_i = \{1_1, .., 1_{L-i-1}, 0_{L-i}, .., 0\}$ (here, the index denotes the corresponding site). These are the components which have all empty sites starting from the first (respectively, last) site up to the i-th ($L - i$-th) and the rest is connected to the left (right) boundary (fig.(15)). The elements ψ_{π_0} and $\psi_{\tilde{\pi}_0}$ are called the fully nested elements (fig.(16)). They play a special role in our computations since all ψ_{π_i} as well as $\psi_{\tilde{\pi}_i}$ can be obtained from the fully nested elements of larger systems using the recurrence relation to which we turn or discussion now.

We notice that when we set two consecutive rapidities z_i and z_{i+1} to $z_i\omega$ and z_i/ω the

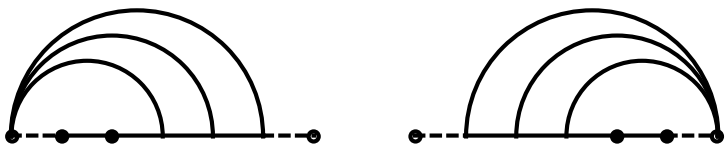

Figure 15: Two link patterns π_2 and $\tilde{\pi}_2$ at $L = 5$.

$\check{R}(z_i, z_{i+1})$ factorizes into two operators

$$\check{R}_i(z\omega, z/\omega) = (\omega^2 + \omega)z^2 S_i M_i. \tag{26}$$

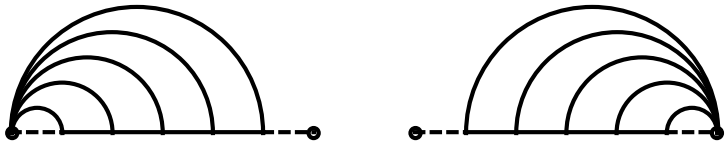

Figure 16: Two $L = 5$ link patterns π_0 and $\tilde{\pi}_0$.

Now using the M_i operator we can write the equation

$$M_i \check{R}_i(t, z_i\omega) R_{i+1}(t, z_i/\omega) = (z_i^2 - t^2) R_i(t, z_i) M_i. \tag{27}$$

This equation means that M maps two sites into one site and hence merges the two R-matrices into one after the substitution $z_i = z_i\omega$ and $z_{i+1} = z_i/\omega$. The graphical representations of M, S and eq.(27) are presented in the figures (17) and (18).

Figure 17: The M_i and S_i operators.

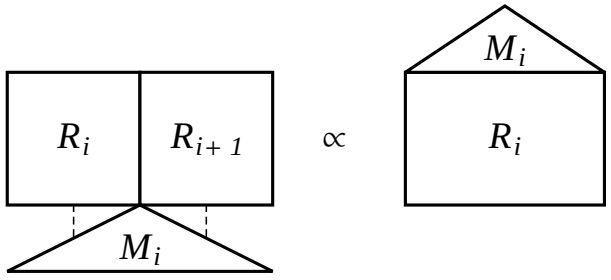

Figure 18: The equation (27).

One can see from the fig.(18) that applying M_i to the transfer matrix we get:

$$M_i T_{L+1}(t|z_1, .., z_i\omega, z_i/\omega, z_{i+1}, .., z_L; \zeta_l, \zeta_r) \propto T_L(t|z_1, .., z_i, z_{i+1}, .., z_L; \zeta_l, \zeta_r) M_i, \tag{28}$$

where we included the indices L and $L+1$ in the transfer matrix to denote the length of the space on which it acts. Applying eq.(28) to the ground state we get:

$$\begin{aligned} &M_i T_{L+1}(.., z_i\omega, z_i/\omega, z_{i+1}, ..) \Psi_{L+1}(.., z_i\omega, z_i/\omega, z_{i+1}, ..) \propto \\ &T_L(.., z_i, z_{i+1}, ..) M_i \Psi_{L+1}(.., z_i\omega, z_i/\omega, z_{i+1}, ..), \end{aligned} \tag{29}$$

which becomes

$$M_i \Psi_{L+1}(.., z_i\omega, z_i/\omega, z_{i+1}, ..) = T_L(t|.., z_i, z_{i+1}, ..) M_i \Psi_{L+1}(.., z_i\omega, z_i/\omega, z_{i+1}, ..), \tag{30}$$

where we omit the dependence on the irrelevant variables for convenience. We obtain the following recurrence relation:

$$M_i \Psi_{L+1}(z_1, .., z_i\omega, z_i/\omega, z_{i+1}, .., z_{L+1}; \zeta_l, \zeta_r) \propto \Psi_L(z_1, .., z_i, z_{i+1}, .., z_L; \zeta_l, \zeta_r). \tag{31}$$

Later on to write this recurrence we will use the operator μ_i that acts on the functions which depend on $z_1, .., z_i, z_{i+1}, .., z_L$ as follows:

$$\mu_i f(z_1, .., z_{i-1}, z_i, z_{i+1}, .., z_j, .., z_L) = f(z_1, .., z_{i-1}, z_i\omega, z_i/\omega, .., z_{j-1}, .., z_{L-1}). \tag{32}$$

The recurrence eq.(31) relates the components of Ψ_{L+1} to the components of Ψ_L. What we need to do to complete this equation is to find the proportionality factor. In the next section we will see that the knowledge of the fully nested element allows to find this proportionality factor. Combining the boundary qKZ equation with eq.(31) will allow us to find all ψ_{π_i}. Then we will show how to recover the full ground state using the qKZ system.

3.1 The qKZ equations and the fully nested elements

Let us take a closer look at the qKZ equations. First we focus on the bulk qKZ. The eq.(23) gives one equation for each link pattern, so 3^L equations in total. It is sufficient to write few distinct cases depending on the local connectivity at the sites i and $i+1$ of a link pattern π of the component ψ_π. For convenience, sometimes we will write $\pi = \{\alpha, n_i, n_{i+1}, \beta\}$, where α and β are respectively the parts of π on the left and on the right to the sites n_i and n_{i+1}, on which we apply the R-matrix in eq.(23). Also, since we will focus only on the sites i and $i+1$ we will not write explicitly the dependence on the variables attached to the other spaces.

1. Both sites i and $i+1$ are occupied.

a.) The sites i and $i+1$ in π are connected via a little arch: $\pi = \{\alpha, 1, -1, \beta\}$. In this case eq.(23) gives:

$$\begin{aligned} &W(z_i, z_{i+1})\psi_\pi(.., z_{i+1}, z_i, ..) = r_9(z_i, z_{i+1})\psi_\pi(.., z_i, z_{i+1}, ..)+ \\ &r_1(z_i, z_{i+1})\psi_{\{\alpha,0,0,\beta\}}(.., z_i, z_{i+1}, ..) + r_8(z_i, z_{i+1}) \sum_{\pi':\rho_i^{(8)}\pi'=\pi} \psi_{\pi'}(.., z_i, z_{i+1}, ..). \end{aligned} \tag{33}$$

b.) The sites i and $i+1$ are not connected to each other:

$$W(z_i, z_{i+1})\psi_\pi(.., z_{i+1}, z_i, ..) = r_9(z_i, z_{i+1})\psi_\pi(.., z_i, z_{i+1}, ..). \tag{34}$$

2. Both sites i and $i+1$ in π are unoccupied

$$\begin{aligned} &W(z_i, z_{i+1})\psi_\pi(.., z_{i+1}, z_i, ..) = r_7(z_i, z_{i+1})\psi_\pi(.., z_i, z_{i+1}, ..)+ \\ &r_3(z_i, z_{i+1}) \sum_{\pi':\rho_i^{(3)}\pi'=\pi} \psi_{\pi'}(.., z_i, z_{i+1}, ..). \end{aligned} \tag{35}$$

3. Finally, one of the sites i and $i+1$ in π is occupied and the other one is unoccupied. There are two distinct cases, in both we will denote by π' the link pattern that is obtained from π by simply interchanging the occupations n_i and n_{i+1} of the sites i and $i+1$ in π. Then, both equations have the same form:

$$W(z_i, z_{i+1})\psi_\pi(.., z_{i+1}, z_i, ..) = r_2(z_i, z_{i+1})\psi_\pi(.., z_i, z_{i+1}, ..) + r_5(z_i, z_{i+1})\psi_{\pi'}(.., z_i, z_{i+1}, ..). \tag{36}$$

This equation corresponds to the case when i is occupied and $i+1$ is empty, the other equation, i.e. the one for i-empty and $i+1$-occupied, is obtained from this one by replacing r_2 with r_4 and r_5 with r_6, however, in both replacements the corresponding weights are equal.

Now let us turn to the boundary qKZ equations. Here, we also have to consider few cases separately. Since the logic is similar for both boundaries we will treat the left boundary only.

1. The first site is occupied.

a.) The connectivity at the first site is $\pi = \{1, \beta\}$, that means that this site is connected to another site or the boundary on the right:

$$U_l(z_1, \zeta_l)\psi_\pi(1/z_1, ..) = k_{l,5}(z_1, \zeta_l)\psi_\pi(z_1, ..). \tag{37}$$

b.) The connectivity at the first site is $\pi = \{-1, \beta\}$, which means it is connected to the left boundary:

$$\begin{aligned} &U_l(z_1, \zeta_l)\psi_\pi(1/z_1, ..) = k_{l,5}(z_1, \zeta_l)\psi_\pi(z_1, ..) + k_{l,1}\psi_{\{0,\beta\}}(z_1, ..)+ \\ &k_{l,4}(\psi_{\{1,\beta\}}(z_1, ..) + \psi_\pi(z_1, ..)), \end{aligned} \tag{38}$$

2. The site 1 is unoccupied $\pi = \{0, \beta\}$:

$$U_l(z_1, \zeta_l)\psi_\pi(1/z_1, ..) = k_{l,3}(z_1, \zeta_l)\psi_\pi(z_1, ..) + k_{l,2}(\psi_{\{1,\beta\}}(z_1, ..) + \psi_{\{-1,\beta\}}(z_1, ..)), \tag{39}$$

As we already mentioned, finding the fully nested elements is the first important step. Let us take a look at the qKZ equations which involve the fully nested elements, i.e. the eq.(34), first for π_0. Let us fix $i = 1$, then this equation after canceling the common factors gives:

$$(\omega z_1 + z_2)\psi_{\pi_0}(z_2, z_1, ..) = (\omega z_2 + z_1)\psi_{\pi_0}(z_1, z_2, ..). \tag{40}$$

This means ψ_{π_0} has the factor $(\omega z_1 + z_2)$ and is symmetric in z_1, z_2 in the remaining part, which we denote by $\psi^{(1)}_{\pi_0}$:

$$\psi_{\pi_0}(z_1, z_2, ..) = (\omega z_1 + z_2)\psi^{(1)}_{\pi_0}(z_1, z_2, ..). \tag{41}$$

Now if we fix $i = 2$ in the equation (34) we see that $\psi^{(1)}_{\pi_0}$ must contain the factor $(\omega z_2 + z_3)$ and taking into account its symmetries it also must contain the factor $(\omega z_1 + z_3)$, we get

$$\psi_{\pi_0}(z_1, z_2, ..) = (\omega z_1 + z_2)(\omega z_2 + z_3)(\omega z_1 + z_3)\psi^{(2)}_{\pi_0}(z_1, z_2, z_3, ..). \tag{42}$$

We can proceed in the same manner for $i = 3, .., L$ and what we obtain in the end is:

$$\psi_{\pi_0}(z_1, z_2, ..) = \psi^{(L-1)}_{\pi_0}(z_1, .., z_L) \prod_{1 \le i < j \le L} (\omega z_i + z_j). \tag{43}$$

Here, $\psi^{(L-1)}_{\pi_0}$ is symmetric in all variables.

The right boundary qKZ equation that involves the ψ_{π_0} (the right boundary analog of eq.(37)) gives:

$$\frac{(-\zeta_r + \zeta_r \omega z_L^2 - z_L)}{\zeta_r z_L}\psi_{\pi_0}(.., 1/z_L) = -\frac{(-\zeta_r \omega + \zeta_r z_L^2 + z_L)}{\zeta_r z_L}\psi_{\pi_0}(.., z_L), \tag{44}$$

which holds when:

$$\psi_{\pi_0}(..,z_L)=\frac{(-\zeta_r+\omega\zeta_r z_L^2-z_L)}{\zeta_r z_L}\bar{\psi}_{\pi_0}(..,z_L), \tag{45}$$

and $\bar{\psi}_{\pi_0}(..,z_L)=\bar{\psi}_{\pi_0}(..,1/z_L)$. At this point it is convenient to reparametrize ζ_r and ζ_l as follows:

$$\zeta_r=\omega\frac{x_r}{x_r^2+1},\quad \zeta_l=\omega\frac{x_l}{x_l^2+1}. \tag{46}$$

Then, equation (45) reads:

$$\psi_{\pi_0}(..,z_L)=\frac{\omega(\omega x_r+z_L)(\omega+x_r z_L)}{x_r z_L}\bar{\psi}_{\pi_0}(..,z_L). \tag{47}$$

Combining this with the eq.(43) we obtain:

$$\psi_{\pi_0}(z_1,z_2,..,z_L;\zeta(z_{L+1}))=\psi^*_{\pi_0}(z_1,..,z_L,z_{L+1})\prod_{1\le i<j\le L+1}\frac{(\omega z_i+z_j)(1+\omega z_i z_j)}{z_i z_j}, \tag{48}$$

where we replaced x_r by z_{L+1}. The prefactor in this expression $\psi^*_{\pi_0}$ is symmetric in all z_i's as well as in $z_i\to z_i^{-1}$. That is all what we can deduce from the qKZ system about the fully nested element ψ_{π_0}. In the same manner we find that:

$$\psi_{\tilde{\pi}_0}(z_1,z_2,..,z_L;\zeta(z_0))=\psi^*_{\tilde{\pi}_0}(z_0,z_1,..,z_L)\prod_{0\le i<j\le L}\frac{(\omega z_i+z_j)(\omega+z_i z_j)}{z_i z_j}. \tag{49}$$

Here z_0 replaces x_l and the prefactor $\psi^*_{\tilde{\pi}_0}$ is symmetric in $\{z_0^{\pm1},z_1^{\pm1},..,z_L^{\pm1}\}$. Both $\psi^*_{\pi_0}$ and $\psi^*_{\tilde{\pi}_0}$ are transparent to the qKZ equations, hence we assume that they do not depend on z_i's.

3.2 The recurrence relation

In this section we are going to complete the equation (31) by deriving the proportionality factor. In order to do that let us figure out first what does the mapping (31) mean for the components of the ground state. This mapping consists of two parts: the action of μ_i and the action of M_i. Since the M_i operator maps the link patterns of size $L+1$ to the link patterns of size L it induces the correspondence of the components of Ψ_{L+1} and Ψ_L. M_i acts on the sites i and $i+1$ by mapping the link patterns of LP_{L+1} with $n_i=1,\ n_{i+1}=-1$ or $n_i=0,\ n_{i+1}=0$ to the link patterns of LP_L with $n_i=0$ and $n_j=n_{j-1}$ for $j>i$, and the remaining unchanged. The link patterns in LP_{L+1} which have $n_i=\pm1,\ n_{i+1}=0$ or $n_i=0,\ n_{i+1}=\pm1$ are mapped to the link patterns of LP_L with $n_i=\pm1$ and $n_j=n_{j-1}$ for $j>i$, and the remaining unchanged (check fig.(19) for example). Note, however, that all components with $n_i=-1,\ n_{i+1}=\pm1$ and $n_i=1,\ n_{i+1}=1$, due to the qKZ equation (34) acquire the factor of $z_i\omega+z_{i+1}$. This factor vanishes under the action of μ_i since $\omega^3=-1$. Therefore, the recurrence (31) implies

$$\mu_i\psi_{n_1,..,n_i=-1,n_{i+1}=\pm1,..,n_{L+1}}(..,z_i,z_{i+1},..)=\mu_i\psi_{n_1,..,n_i=1,n_{i+1}=1,..,n_{L+1}}(..,z_i,z_{i+1},..)=0, \tag{50}$$

$$\mu_i\psi_{n_1,..,n_i=1,n_{i+1}=-1,..,n_{L+1}}(..,z_i,z_{i+1},..)=F_i(z_1,..,z_L)\psi_{n_1,..,n_i=0,..,n_L}(..,z_i,..), \tag{51}$$

$$\mu_i\psi_{n_1,..,n_i=1,n_{i+1}=0,..,n_{L+1}}(..,z_i,z_{i+1},..)=F_i(z_1,..,z_L)\psi_{n_1,..,n_i=1,..,n_L}(..,z_i,..), \tag{52}$$

$$\mu_i\psi_{n_1,..,n_i=0,n_{i+1}=1,..,n_{L+1}}(..,z_i,z_{i+1},..)=F_i(z_1,..,z_L)\psi_{n_1,..,n_i=1,..,n_L}(..,z_i,..), \tag{53}$$

$$\mu_i\psi_{n_1,..,n_i=0,n_{i+1}=0,..,n_{L+1}}(..,z_i,z_{i+1},..)=F_i(z_1,..,z_L)\psi_{n_1,..,n_i=0,..,n_L}(..,z_i,..). \tag{54}$$

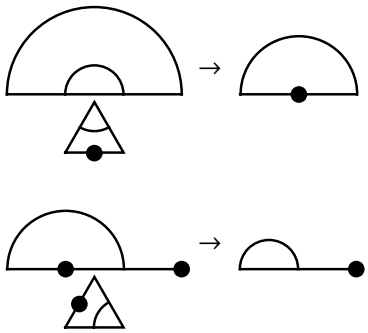

Figure 19: The action of the M_2 operator.

Here, for the compactness we omitted the dependence on the z_j's $j \neq i,\ j \neq i+1$ which are unimportant in the recurrence relation. The factor $F_i(z_1, .., z_L)$ is exactly the proportionality factor in the eq.(31), and the label i denotes the site on which μ_i recurrence is applied. F_i also depends on the ζ_l and ζ_r which we did not indicate explicitly.

Now we would like to obtain the explicit form of the F_i. In order to do that we need to consider the left boundary qKZ equation for the element ψ_{π_0} which is given by eq.(38) and apply twice the μ_1 operator to this equation. Here is what we get:

$$\mu_1 U_l(z_1, \zeta_l)\psi_{\pi_0}(1/z_1, .., z_{L+2}) = \mu_1 k_{l,5}(z_1, \zeta_l)\psi_{\pi_0}(z_1, .., z_{L+2}) + \\ \mu_1 k_{l,1}(z_1, \zeta_l)\psi_{\pi_1}(z_1, .., z_{L+2}) + \mu_1 k_{l,4}(z_1, \zeta_l)(\psi_{\{1,-1..,-1\}}(z_1, .., z_{L+2}) + \psi_{\pi_0}(z_1, .., z_{L+2})). \quad (55)$$

Using the eq.(50), eq.(53) and eq.(51) we obtain:

$$U_l(z_1\omega, \zeta_l)\psi_{\pi_0}(1/(z_1\omega), z_1/\omega, z_2, .., z_{L+1}) = \\ F_1(z_1, .., z_{L+1})(k_{l,1}(z_1\omega, \zeta_l)\psi_{\pi_0}(z_1, .., z_{L+1}) + k_{l,4}(z_1\omega, \zeta_l)\psi_{\pi_1}(z_1, .., z_{L+1})). \quad (56)$$

Applying μ_1 again we arrive at an equation containing the F's and the fully nested elements:

$$U_l(z_1\omega^2, \zeta_l)\psi_{\pi_0}(1/(z_1\omega^2), z_1, z_1/\omega, z_2, .., z_L) = \\ F_1(z_1\omega, z_1/\omega, .., z_L)F_1(z_1, .., z_L)k_{l,4}(z_1\omega^2, \zeta_l)\psi_{\pi_0}(z_1, .., z_L). \quad (57)$$

Plugging here the explicit form of ψ_{π_0} we find that:

$$F_i(z_1, .., z_L; \zeta_l(z_0), \zeta_r(z_{L+1})) = \prod_{0 \leq j \neq i \leq L+1} \frac{(z_i + z_j)(z_i z_j + 1)}{z_i z_j} \quad (58)$$

satisfies the eq.(57) with $i = 1$, provided we choose appropriately the constant $\psi^*_{\pi_0}$. Although we computed (58) for $i = 1$, it is also true for $i > 1$. One can see that by looking at this recurrence relation for the special case of the component which has all $n_i = 0$.

3.3 Computation of the ψ_{π_i} components

So far we know only the fully nested elements ψ_{π_0} and $\psi_{\tilde{\pi}_0}$. The only qKZ equation that relates the fully nested element with others is (38), however, it has two unknowns: $\psi_{\{1,-1..,-1\}}$ and $\psi_{\pi_1} = \psi_{\{0,-1,..,-1\}}$. As we already saw, after the action of μ_1 one of the two unknowns in

(38) disappear and we arrive at (56), hence we can express the element ψ_{π_1} in terms of ψ_{π_0} and the equation (38) gives us the second unknown $\psi_{\{1,-1..,-1\}}$.

In general, the equation (56) holds if we replace π_0 by $\pi = \{-1,-1,\alpha\}$ for any α. The equation (56) then maps the component $\psi_{\{-1,-1,\alpha\}}$ and $\psi_{\{-1,\alpha\}}$ of the ground state Ψ_{L+1} and Ψ_L (respectively) to the components $\psi_{\{0,\alpha\}}$ of the ground state Ψ_L:

$$\psi_{\{0,\alpha\}}(z_1,z_2,..,z_L)) = k_{l,4}^{-1}(z_1\omega,\zeta_l)\Bigg(U_l(z_1\omega,\zeta_l)\frac{\psi_{\{-1,-1,\alpha\}}(1/(z_1\omega),z_1/\omega,z_2,..,z_L)}{F_1(z_1,..,z_L)} + k_{l,1}(z_1\omega,\zeta_l)\psi_{\{-1,\alpha\}}(z_1,z_2,..,z_L)\Bigg). \tag{59}$$

This equation is the first important ingredient in the computation of ψ_{π_i}. The second ingredient is the equation (36) which allows to compute the component $\psi_{\{\alpha,0,\pm1,\beta\}}$ if the component $\psi_{\{\alpha,\pm1,0,\beta\}}$ is known and vice versa. The latter means all components with a fixed relative connectivity of the lines (relative positions of $+1$'s and -1's in π) form an equivalence class w.r.t. the operators (see fig.(20)):

$$\eta_i = \frac{W(z_i,z_{i+1})}{r_5(z_i,z_{i+1})}(\tau_i - 1) + 1, \tag{60}$$
$$\text{where} \quad \tau_i f_(..,z_i,z_{i+1},..) = f(..,z_{i+1},z_i,..),$$

thus, we get the identities:

$$\psi_{\{\alpha,\pm1_i,0_{i+1},\beta\}} = \eta_i \psi_{\{\alpha,0_i,\pm1_{i+1},\beta\}}, \tag{61}$$
$$\psi_{\{\alpha,0_i,\pm1_{i+1},\beta\}} = \eta_i \psi_{\{\alpha,\pm1_i,0_{i+1},\beta\}}. \tag{62}$$

Plugging $\eta_1\psi_{\pi_1}(z_1,..,z_L)$ and $\eta_2\eta_1\psi_{\pi_1}(z_1,..,z_{L+1})$ into (59) gives ψ_{π_2}. It is clear now that by substituting:

$$\psi_{\{-1,\alpha\}}(z_1,..,z_L) = \prod_{k=0}^{i-1}\eta_{i-k}\psi_{\pi_i}(z_1,..,z_L), \tag{63}$$

$$\psi_{\{-1,-1,\alpha\}}(z_1,..,z_{L+1}) = \prod_{k=0}^{i-1}\eta_{i-k+1}\eta_{i-k}\psi_{\pi_i}(z_1,..,z_{L+1}), \tag{64}$$

into the eq.(59) we can inductively obtain all ψ_{π_i}. Note, that the eq.(38) for $\pi = \{-1,-1,\alpha\}$ where α contains 0's and/or -1's allows to obtain all elements ψ_π with $\pi = \{1,-1,\alpha\}$. Using η_i's we also get all elements in the equivalence of $\psi_{\{1,-1,\alpha\}}$. Now we can turn to the computation of the other elements of the ground state Ψ_L.

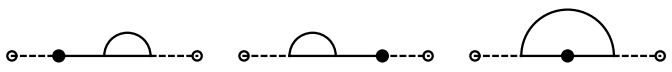

Figure 20: Equivalence class of the element $\pi = \{0,1,-1\}$.

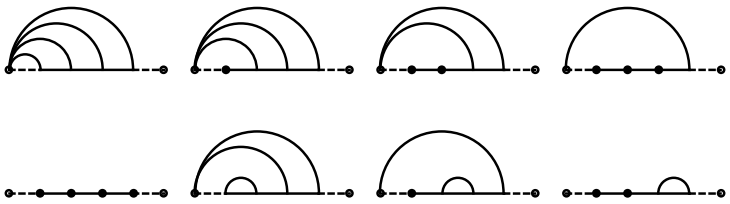

Figure 21: Elements corresponding to nonequivalent link patterns of the elements of Ψ_4 can be computed using only the equations (56), (38), (63) and (64).

3.4 Dyck paths and the ground state components

As in [11], a good way to see how the components of Ψ_L can be computed is to turn to the Dyck path formulation. The set of link patterns of length L is the set $\mathbb{Z}_3^{\otimes L}$. To any π we associate a unique Dyck path in the following way. Reading π from left to right every 1 in π will be a north east (NE) step, every -1 in π will be a south east (SE) step and every 0 will be a horizontal east (E) step. For example, the link pattern $\{-1,-1,0,1,1,0,0,-1,-1,1\}$ is represented by the {SE,SE,E,NE,NE,E,E,SE,SE,NE} Dyck path as in fig.(22). A few

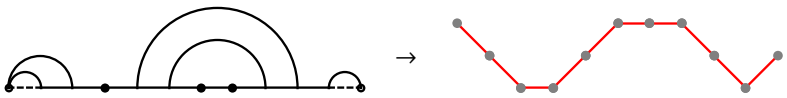

Figure 22: The $\{-1,-1,0,1,1,0,0,-1,-1,1\}$ link pattern and the corresponding Dyck path. The ending and the beginning of each step in the Dyck path is marked by a small disk on the picture.

distinguished Dyck paths are those which correspond to the fully nested link patterns (see fig.(23)). The area under the Dyck paths can be split into few boundary triangles $t_{l,1}$, $t_{l,2}$,

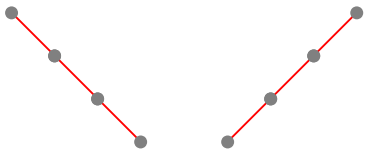

Figure 23: The Dyck paths of $\pi = \{-1,-1,-1\}$ and $\tilde{\pi} = \{1,1,1\}$.

$t_{r,1}$ and $t_{r,2}$, bulk triangles $t^{(1)}$ and $t^{(2)}$ and lozenges $l^{(1)}$ and $l^{(2)}$ depicted on the fig.(24). Note, that we need to supplement the bulk triangles and lozenges with an index j, then by $t_j^{(i)}$ and $l_j^{(i)}$ we will denote the operator $t^{(i)}$, respectively $l^{(i)}$, acting at the position j. Each Dyck path can be build by concatenation of these primitives starting from a reference Dyck path. For example, if the reference Dyck path is $\pi_e = \{0,0,..,0\}$ the Dyck path $\pi = \{-1,-1,0,1,1,0,0,-1,-1,1\}$, depicted on the fig.(25), is constructed, e.g. as follows

$$\pi = t_6^{(2)} t_7^{(1)} t_5^{(1)} t_{1,l} t_7^{(2)} t_5^{(2)} t_{2,l} t_1^{(1)} t_4^{(1)} t_6^{(1)} t_8^{(1)} t_{1,r} \pi_e. \tag{65}$$

Similarly, as one link pattern can be converted into another upon the action of a product of ρ_i operators, one Dyck path can be converted into another one by attaching or removing rhombi $l^{(i)}$ and triangles $t^{(i)}$ and $t_{i,l/r}$.

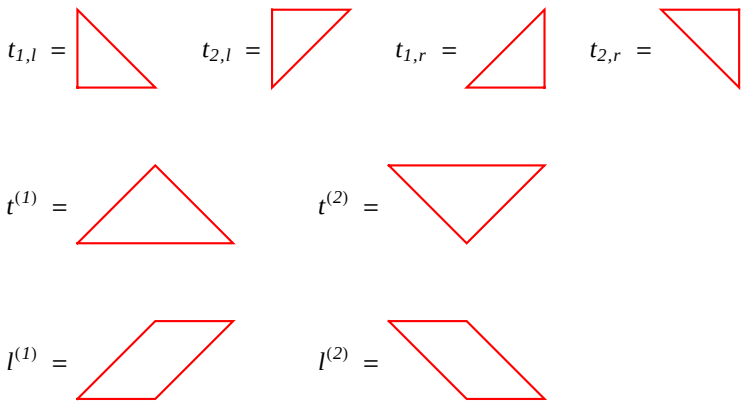

Figure 24: The left boundary $t_{1,l}$, $t_{2,l}$, right boundary $t_{1,r}$, $t_{2,r}$, the bulk $t^{(1)}$, $t^{(2)}$ triangles and the bulk rhombi $l^{(1)}$, $l^{(2)}$.

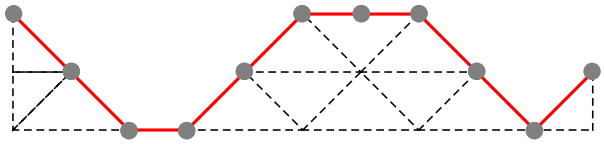

Figure 25: A decomposition of the Dyck path $\{-1,-1,0,1,1,0,0,-1,-1,1\}$.

Now we introduce the notion of partial ordering on the Dyck Paths. A path π_1 is contained in another path π_2: $\pi_1 \prec \pi_2$ if π_1 can be completed to π_2 by adding to it triangles and lozenges. To make this notion less ambiguous we need to indicate, for example, what is the largest Dyck path w.r.t. all other Dyck paths. Let us choose the element π_0 to be the largest, then the smallest element will be $\tilde{\pi}_0$. This means that the addition of the triangles or lozenges to the element π_0 is forbidden as well as the removal of the triangles or lozenges from the element $\tilde{\pi}_0$, hence all Dyck paths are contained in the region surrounded by the triangle $D_L = \{\{0,L\},\{L,0\}\,\{0,-L\}\}$. This region D_L is depicted on the fig.(26).

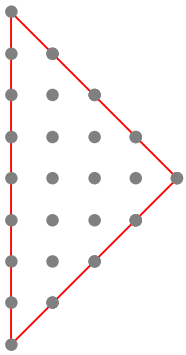

Figure 26: The domain D_L. The gray disks represent the nodes which the possible Dyck paths may visit.

In order to compute the remaining elements of the ground state we will need the eq.(35),

which we rewrite in the following form for $\pi = \{\alpha, 0, 0, \beta\}$:

$$\delta_i \psi_{\{\alpha,0,0,\beta\}}(.., z_i, z_{i+1}, ..) - \psi_{\{\alpha,1,-1,\beta\}}(.., z_i, z_{i+1}, ..) = \sum_{\substack{\pi' : \rho_i^{(8)} \pi' = \pi \\ \pi' \neq \pi}} \psi_{\pi'}(.., z_i, z_{i+1}, ..), \tag{66}$$

where we defined the operator δ_i:

$$\delta_i = \frac{W(z_i, z_{i+1})\tau_i - r_7(z_i, z_{i+1})}{r_1(z_i, z_{i+1})}. \tag{67}$$

The boundary qKZ with $\pi = \{0, \alpha\}$ (39) is also useful to rewrite as:

$$\gamma_l \psi_{\{0,\alpha\}}(z_1, ..) - \psi_{\{1,\alpha\}}(z_1, ..) = \psi_{\{-1,\alpha\}}(z_1, ..), \tag{68}$$

where we defined the operator γ_l:

$$\gamma_l = \frac{U_l(z_1, \zeta_l)\sigma_l - k_{l,3}(z_1, \zeta_l)}{k_{l,2}(z_1, \zeta_l)}, \quad \text{and} \quad \sigma_l f(z_1, z_2, ..) = f(1/z_1, z_2, ..). \tag{69}$$

Note, in both equations (66) and (68) in the right hand sides we can identify the smallest elements in those equations in the sense of the ordering of Dyck paths. The idea below is to compute one by one elements ψ_π in the direction of decreasing π, therefore equations (66) and (68) will always have one unknown which will be the element corresponding to the smallest π in them.

We are going to proceed as follows. Let us consider the elements corresponding to the Dyck paths passing through the points $\{j, L-j\}$ for $0 \leq j \leq L$, i.e. the points on the right boundary of the domain D_L. Take $j = 0$, there is only one path which passes through this point and it corresponds to ψ_{π_0}. Next we take $j = 1$, there are two paths corresponding to ψ_1 and ψ_2 on the fig.(27). Next we take $j = 2$, these paths are labeled by ψ_i with $i = 3, .., 8$ on the fig.(27). The already known components are ψ_0, ψ_1, ψ_2, ψ_3 and ψ_4. Every unknown

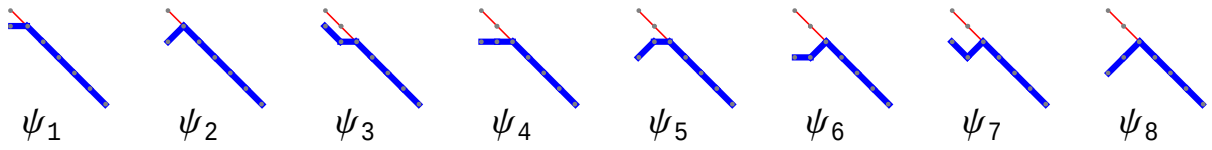

Figure 27: The Dyck paths (thick blue line) passing the $\{1, L-1\}$ point (ψ_1 and ψ_2) and the Dyck paths passing the point $\{2, L-2\}$ (ψ_j, $j = 3, .., 8$) of the domain D_L. Here, for reference we also included the north to east edge of the D_L triangle.

ψ_i on this figure we can obtain from a few ψ_j's with $j < i$ and $\psi_0 = \psi_{\pi_0}$. Indeed, we have:

$$\psi_5 = \gamma_l \psi_4 - \psi_3, \quad \psi_6 = \eta_1 \psi_5, \quad \psi_7 = \delta_1 \psi_4 - \psi_2 - \psi_0, \quad \psi_8 = \gamma_l \psi_6 - \psi_7. \tag{70}$$

Let us take now $j = 3$, the Dyck paths passing through this point are depicted on the fig.(28). From these we already know the components which are in the equivalence class of ψ_i's from

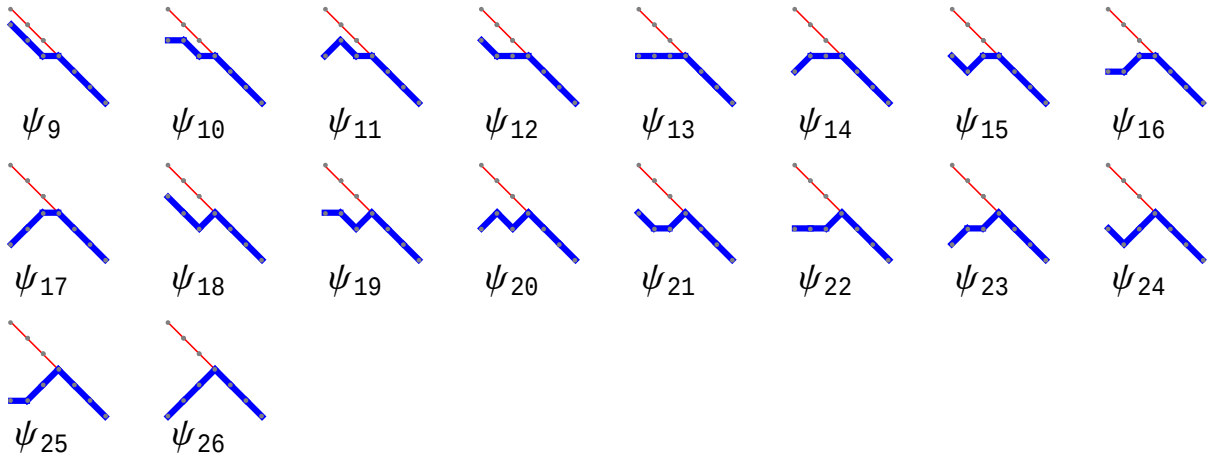

Figure 28: Dyck paths passing the $\{3, L-3\}$ point of the domain D_L.

the fig.(27) and ψ_{π_i}, these components are: ψ_9, ψ_{10}, ψ_{11}, ψ_{12}, ψ_{13}, the rest are:

$$\begin{aligned}
&\psi_{14} = \gamma_l\psi_{13} - \psi_{12}, \quad \psi_{15} = \delta_1\psi_{13} - \psi_{11} - \psi_9, \quad \psi_{16} = \eta_1\psi_{14}, \quad \psi_{17} = \gamma_l\psi_{16} - \psi_{15},\\
&\psi_{18} = \delta_2\psi_{12} - \psi_7 - \psi_0, \quad \psi_{19} = \eta_1\eta_2\psi_{15}, \quad \psi_{20} = \gamma_l\psi_{19} - \psi_{18}, \quad \psi_{21} = \eta_1\psi_{15},\\
&\psi_{22} = \eta_2\eta_1\psi_{14}, \quad \psi_{23} = \gamma_l\psi_{22} - \psi_{21}, \quad \psi_{24} = \delta_1\psi_{22} - \psi_{18} - \psi_{20} - \psi_8,\\
&\psi_{25} = \eta_1\eta_2\psi_{17}, \quad \psi_{26} = \gamma_l\psi_{25} - \psi_{24}.
\end{aligned} \tag{71}$$

These computations are valid for any L larger or equal to 3. In the latter case it gives all 27 components. From the beginning of the computation we have chosen the reference state to be ψ_{π_0} which is associated to the left boundary. We then observed that any component ψ_π can be expressed through a number of components associated to larger Dyck paths than the path π. All computations can be done in a similar manner using for the reference $\psi_{\bar{\pi}_0}$. The explicit results for $L = 1, 2$ are presented in the appendix A.

4 Discussions

Usually, integrable models at finite size are studied via the Bethe ansatz, in which case the eigenstates of the transfer matrix depend on the Bethe roots. One then has to solve the set of nonlinear Bethe equations in order to obtain the eigenstates and the eigenvalues. In our case, following the prescription developed for the TL model at $n = 1$ [12], we were able to find the ground state eigenvector explicitly for finite systems avoiding the complicated nonlinear equations. Indeed, if we take our ground state Ψ_L in the spin basis (which amounts to a linear transformation on Ψ_L, see e.g. [21]) this will correspond to the ground state of the 19 vertex Izergin-Korepin (IK) model at $q^3 = -1$. The algebraic Bethe ansatz for this model with periodic boundary conditions was found by Tarasov [25]. By substituting the Bethe roots in the ground state in the algebraic Bethe ansatz for the 19 vertex IK model with periodic boundary conditions we verified the ground state results obtained for dTL on a cylinder.

The approach that we are using allows to find (strictly speaking to conjecture) closed expressions for a few components of the ground state vector. These components are the fully

nested element ψ_{π_0} and few others which are "close" enough to ψ_{π_0} and expressed through the ψ_{π_0} itself, e.g. ψ_{π_1} from the eq.(59). As we go "down" in the triangle D_L the complexity of the computations increases rapidly, that is why we are limited to only few components. Another component which we can write in a closed form for arbitrary L is ψ_e. It turns out that this component is proportional to Z_L-the sum of all components of Ψ_L. Z_L is the normalization of the ground state Ψ_L, thus it is an important quantity for the computation of correlation functions. One such correlation function is the boundary to boundary current. It was computed for the TL model in [6] and in our case it is the subject of the paper [9]. Due to the relation of the dilute TL model at $n = 1$ to the critical site percolation, Z_L^2 plays the role of the partition function in the critical percolation on an infinite strip. We compute Z_L in [15].

We would like to stress here that we were dealing with the generic open boundary conditions. In this case the boundaries carry the parameters ζ_l and ζ_r. Sending a ζ to 0 (with the proper normalization) from our Ψ_L we recover the ground state Ψ_L^c of the loop model with closed (also called reflecting) boundary conditions. In this case one could study an interesting correlation function: the current going from $-\infty$ to $+\infty$ along the strip. This current was studied in the paper [16] for the TL $n = 1$ loop model. One could also send a ζ to infinity (with a proper normalization), then the corresponding K-matrix is a combination of κ_3, κ_4 and κ_5. This can be an interesting case to study, since as it is stressed in [5] there are few solutions $K^{(1)}$ and $K^{(2)}$ to the reflection equation. The solution $K^{(1)}$ is the one we used here. The solution $K^{(2)}$ is a combination of only three operators κ_3, κ_4 and κ_5. The two solutions are independent for generic n, but for $n = 1$ $K^{(2)}$ is the $\zeta \to \infty$ limit of $K^{(1)}$. Hence to compute the ground state with $K^{(2)}$-matrix one needs to send ζ to infinity in our solution.

The next point we would like to stress is the computation of the ground state at $n = 0$. It turns out that at this point the dilute TL loop model also possesses a polynomial ground state and the qKZ together with the recurrence relations remain intact. Few qKZ equations, however, modify, but this does not change much the algorithm of the computation of Ψ_L presented here.

Acknowledgements

A. G. was supported by the ERC grant 278124 "Loop models, Integrability and Combinatorics" and AMS Amsterdam Scholarship. A. G. thanks the University of Amsterdam for hospitality and P. Zinn-Justin and G. Fehér for useful discussions.

Appendix A

We present in this appendix the explicit expressions for the polynomial ground state Ψ_L for $L = 1,\ 2$. The Ψ_1 components are:

$$\psi_{-1} = \frac{\omega\,(x_r + \omega z_1)\,(\omega z_1 x_r + 1)}{z_1 x_r}, \tag{72}$$

$$\psi_1 = \frac{\omega\,(\omega x_l + z_1)\,(z_1 x_l + \omega)}{z_1 x_l}, \tag{73}$$

$$\psi_0 = \frac{\omega^2\,(z_1 x_l^2 x_r + z_1^2 x_l x_r + z_1 x_l x_r^2 + x_l x_r + z_1 x_l + z_1 x_r)}{z_1 x_l x_r}. \tag{74}$$

The last component can be written in terms of the elementary symmetric polynomials

$$E_m(z_1, .., z_L) = \sum_{1 \le i_1 < ,.., < i_m} z_{i_1} .. z_{i_m},$$
$$E_m(z_1, .., z_L) = 0 \quad \text{for} \quad m < 0, \quad \text{and} \quad m > L,$$

as follows:

$$\psi_0(z_1; x_l, x_r) = \frac{\omega^2 (E_2 + E_1 E_3)}{E_3}, \tag{75}$$

in which $E_i = E_i(x_l, z_1, x_r)$. The choice of the constant prefactor of the nested elements in (72) and (73) fixes the constants $\psi^*_{\pi_0}$ and $\psi^*_{\tilde{\pi}_0}$ from eq.(48) and eq.(49). Hence we will not write the nested elements for $L = 2$. The rest of the components of Ψ_2 up to a η_i action are:

$$\psi_{1,-1} = \frac{(\omega x_l + z_1)\,(z_1 x_l + \omega)\,(x_r + \omega z_2)\,(\omega z_2 x_r + 1)}{z_1^2 z_2^2 x_l^2 x_r^2}(E_3 + E_1 E_4),$$

$$\psi_{0,-1} = \frac{\omega\,(x_r + \omega z_2)\,(\omega z_2 x_r + 1)}{z_1^2 z_2^2 x_l x_r^2}\Big(z_1(1 + z_2^2)(E_2(x_l, z_1, x_r) + E_1(x_l, z_1, x_r) E_3(x_l, z_1, x_r)) +$$

$$z_2\big(\left(z_1^2 + 1\right) x_l\,(x_r + z_1)\,(z_1 x_r + 1) + z_1(x_1^2 + 1)\left((\omega + 1) x_r\left(\omega^2 + z_1^2\right) + z_1(x_r^2 + 1)\right)\big)\Big),$$

$$\psi_{1,0} = \frac{\omega\,(\omega x_l + z_1)\,(z_1 x_l + \omega)}{z_1^2 z_2^2 x_l^2 x_r}\Big(z_2(1 + z_1^2)(E_2(x_l, z_2, x_r) + E_1(x_l, z_2, x_r) E_3(x_l, z_2, x_r)) +$$

$$z_1\big(z_2\left(x_l^2 + 1\right)(x_r + z_2)\,(z_2 x_r + 1) + x_l\left((\omega + 1) z_2\left(x_r^2 + 1\right)\left(\omega^2 z_2^2 + 1\right) + \left(z_2^2 + 1\right)^2 x_r\right)\big)\Big),$$

$$\psi_{-1,1} = \frac{\omega(\omega + 1)\,(z_1 z_2 + 1)\,(\omega z_1 + z_2)}{z_1^2 z_2^2 x_l x_r}\Big((\omega + 1) x_l x_r(1 + z_1^2 z_2^2) +$$
$$(z_1 + z_2)(\omega x_l x_r^2 + x_l^2 x_r + \omega x_l + x_r) + (\omega + 1) z_1 z_2\left(x_l^2 x_r^2 + x_l x_r + x_l^2 + x_r^2 + 1\right) +$$
$$z_1 z_2\,(z_1 + z_2)\left(\omega x_l^2 x_r + x_l x_r^2 + x_l + \omega x_r\right)\Big),$$

$$\psi_{0,0} = \frac{\omega^2}{E_4^2}(E_3 + E_1 E_4)(E_2 - E_4 + E_1 E_3 + E_2 E_4). \tag{76}$$

In these equations when the arguments of E_i are not specified we imply $E_i = E_i(x_l, z_1, z_2, x_r)$.

Appendix B

In this appendix we discuss in more detail the equation (27) (see also fig.(18). When the argument of the matrix $R(z)$ is equal to ω^2 the weight ρ_9 in eq.(18) vanishes, and the R-matrix can be split into a product of two operators shown on fig.(17). Now we take M operator and substitute it into the equation fig.(18). The left hand side of this equation is shown on fig.(29), while the right hand side is shown on fig.(30). On both sides we have five

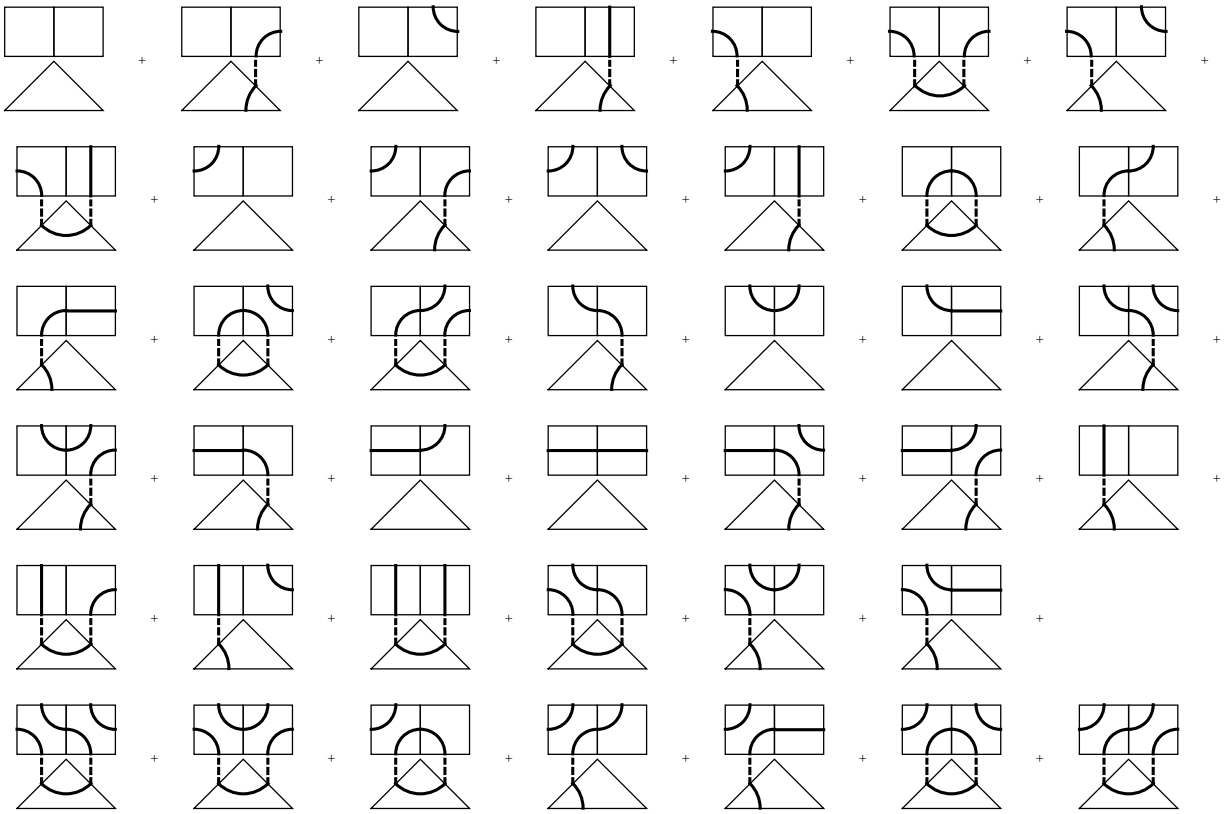

Figure 29: The left hand side of (18). The weights of each term here are the products of the weights of the constituting operators.

external edges. The sum of the weights of the terms with the same connectivity on the left hand side must be equal to the sum of the weights of the terms with the same connectivity on the right hand side times the factor $(t^2 - z_i^2)$. For example, if we take the terms with all five external edges empty on the left hand side, which is two terms: the one with no lines in the interior of the diagram and the one with a loop in the interior, this will give the weight $(t^2 - z_i^2)^2$. This is equal to the weight $\rho_7(t, z_i)$ times the factor $(t^2 - z_i^2)$, which is in agreement with the computation on the right hand side. In particular, all terms on the left hand side which have two top horizontal edges occupied and not connected cancel each other since such a connectivity is absent on the right hand side. It is a straightforward but a lengthy computation to check that (27) holds.

The factorization property of the R matrix holds for generic values of q. In this case the empty plaquette of the M operator will acquire the weight of n and the same for the S operator. The derivation of this fact will appear elsewhere [14]. In the context of quantum

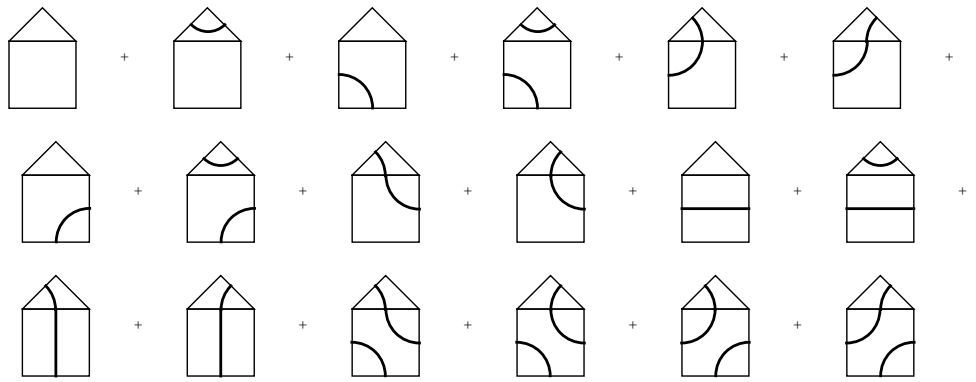

Figure 30: The right hand side of the equation (18). The weights of each term here are the products of the weights of the constituting operators.

groups this factorization of the R-matrix is related to the quasi-triangularity property which is one of the defining properties of the quasi-triangular Hopf algebras [23].

References

[1] M. T. Batchelor, J. de Gier, and B. Nienhuis. The quantum symmetric XXZ chain at $\Delta = -\frac{1}{2}$, alternating-sign matrices and plane partitions. *J. Phys. A*, 34:L265–L270, 2001.

[2] R. J. Baxter. *Exactly solved models in statistical mechanics*. academic Press Inc. [Harcourt Brace Jovanovich], London, 1982.

[3] L. Cantini. qKZ equation and ground state of the O(1) loop model with open boundary conditions. *arXiv: 0903. 5050*, 2009.

[4] L. Cantini and A. Sportiello. Proof of the Razumov-Stroganov Conjecture. *J. Comb. Theory Ser. A*, 118(5):1549–1574, 2011.

[5] J. de Gier, A. Lee, and J. Rasmussen. Discrete holomorphicity and integrability in loop models with open boundaries. *J.Stat.Mech.*, 1302:P02029, 2013.

[6] J. de Gier, B. Nienhuis, and A. Ponsaing. Exact spin quantum Hall current between boundaries of a lattice strip. *Nuclear Physics B*, 838(3):371–390, 2010.

[7] J. de Gier, A. Ponsaing, and K. Shigechi. The exact finite size ground state of the O(n = 1) loop model with open boundaries. *Journal of Statistical Mechanics: Theory and Experiment*, 2009(04):P04010, 2009.

[8] J. Dubail, J. L. Jacobsen, and H. Saleur. Conformal boundary conditions in the critical O(n) model and dilute loop models. *Nucl.Phys.*, B827:457–502, 2010.

[9] G. Fehér and B. Nienhuis. Currents in the dilute O($n = 1$) loop model. Unpublished, 2014.

[10] P. Di Francesco. unpblished notes.

[11] P. Di Francesco. Inhomogeneous loop models with open boundaries. *Journal of Physics A: Mathematical and General*, 38(27):6091, 2005.

[12] P. Di Francesco and P. Zinn-Justin. Inhomogenous model of crossing loops and multidegrees of some algebraic varieties. *arXiv: math-ph/ 0412031*, 2004.

[13] A. Garbali. Dilute O(1) Loop Model on a Strip and the qKZ Equations. `http://www.science.uva.nl/onderwijs/thesis/centraal/files/f1958551609.pdf`, 2012. Master Thesis, University of Amsterdam.

[14] A. Garbali. PhD thesis: Some aspects of the $U_q(A_2^{(2)})$ and $U_q(A_1^{(1)})$ integrable models. Unpublished, 2015.

[15] A. Garbali and B. Nienhuis. The dilute Temperley-Lieb O($n = 1$) loop model on a semi infinite strip: the sum rule. Unpublished, 2014.

[16] Y. Ikhlef and A. K. Ponsaing. Finite-Size Left-Passage Probability in Percolation. *Journal of Statistical Physics*, 149(1):10–36.

[17] A. Knutson and P. Zinn-Justin. The Brauer loop scheme and orbital varieties. *arXiv: 1001. 3335*, 2010.

[18] S. Mitra and B. Nienhuis. Exact conjectured expressions for correlations in the dense O(1) loop model on cylinders. *Journal of Statistical Mechanics: Theory and Experiment*, 2004(10):P10006, 2004.

[19] S. Mitra, B. Nienhuis, J. de Gier, and M. T. Batchelor. Exact expressions for correlations in the ground state of the dense O(1) loop model. *Journal of Statistical Mechanics: Theory and Experiment*, 2004(09):P09010, 2004.

[20] B. Nienhuis. Critical and multicritical O(n) models. *Physica A*, 163:152–157, 1990.

[21] B. Nienhuis. Critical spin-1 vertex models and O(n) models. *Int. J. Mod. Phys. B*, 4:929–942, 1990.

[22] A.V. Razumov and Yu. G. Stroganov. Combinatorial nature of ground state vector of O(1) loop model. *Theor. Math. Phys.*, 137:333–337, 2004.

[23] S. Montgomery. *Hopf algebras and their actions on rings. Expanded version of ten lectures given at the CBMS Conference on Hopf algebras and their actions on rings, which took place at DePaul University in Chicago, USA, August 10-14, 1992.* Providence, RI: American Mathematical Society, 1993.

[24] E. K. Sklyanin. Boundary conditions for integrable quantum systems. *J. Phys. A*, 21:2375–2389, 1988.

[25] V. O. Tarasov. Algebraic Bethe ansatz for the Izergin-Korepin R-matrix. *Theor. Math. Phys.*, 76:793–803, 1988.

[26] P. Zinn-Justin. Loop model with mixed boundary conditions, qKZ equation and alternating sign matrices. *Journal of Statistical Mechanics: Theory and Experiment*, 2007(01):P01007, 2007.